

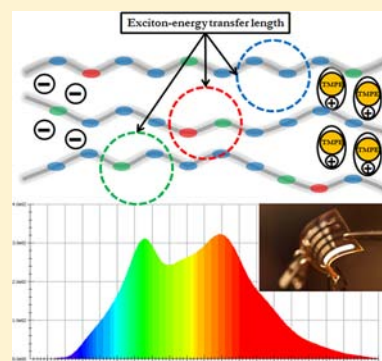
# White Light from a Single-Emitter Light-Emitting Electrochemical Cell

Shi Tang,<sup>†</sup> Junyou Pan,<sup>‡</sup> Herwig A. Buchholz,<sup>‡</sup> and Ludvig Edman<sup>\*,†</sup>

<sup>†</sup>The Organic Photonics and Electronics Group, Department of Physics, Umeå University, SE-901 87 Umeå, Sweden

<sup>‡</sup>Merck KGaA, Frankfurter Str. 250, 64293 Darmstadt, Germany

**ABSTRACT:** We report a novel and generic approach for attaining white light from a single-emitter light-emitting electrochemical cell (LEC). With an active-layer comprising a multifluorophoric conjugated copolymer (MCP) and an electrolyte designed to inhibit MCP energy-transfer interactions during LEC operation, we are able to demonstrate LECs that emit broad-band white light with a color rendering index of 82, a correlated-color temperature of 4000 K, and a current conversion efficacy of 3.8 cd/A. It is notable that this single-emitter LEC configuration eliminates color-drift problems stemming from phase separation, which are commonly observed in conventional blended multiemitter devices. Moreover, the key role of the electrolyte in limiting undesired energy-transfer reactions is highlighted by the observation that an electrolyte-free organic light-emitting diode comprising the same MCP emits red light.



## 1. INTRODUCTION

White light emission from a large-area, and in some cases conformable, surface is a highly attractive concept for a wide range of incumbent and futuristic display and solid-stage lighting applications. This feature is also currently becoming offered by organic light-emitting diode (OLED)<sup>1</sup> and light-emitting electrochemical cell (LEC)<sup>2</sup> technologies, which utilize conjugated small molecules or polymers for the emitting species. The two most common enabling approaches for broad-band white emission are the employment of a multilayer geometry,<sup>3–5</sup> comprising stacked layers of complementary emitting materials, and a single-layer blend-emitter geometry,<sup>6–10</sup> comprising a blended multicomponent emitter system.

The multilayer approach has demonstrated efficient and stable performance in vacuum-fabricated OLEDs<sup>11</sup> but is unfortunately difficult to realize with low-cost solution-based fabrication processes, as the solvents utilized for the deposition of the upper layer(s) commonly dissolve and/or damage the underneath layer(s). The single-layer blend-emitter approach, on the other hand, is compatible with solution processing (today most commonly spin-coating)<sup>12–14</sup> but instead suffers from stability problems stemming from a tendency of the different emitters to phase separate during operation and a concomitant undesired voltage- and/or time-induced color shift.<sup>15–18</sup> A practical solution to the above shortcomings is the employment of a single-layer active material comprising a multifluorophoric conjugated polymer (MCP) as a broad-band single emitter. This concept was introduced in an OLED by Lee and co-workers in 2005,<sup>19</sup> and several other research groups have since developed such white-emitting OLED devices.<sup>20–26</sup>

The LEC is an often overlooked alternative to the OLED, with the nominal difference being that the LEC comprises an

electrolyte (mobile ions) blended into the active layer.<sup>2,27–33</sup>

The mobile ions reorganize and infiltrate the light-emitting material when a voltage is applied, so that a light-emitting p–n junction doping structure can form *in situ* in the active layer.<sup>34–36</sup> This doping process paves the way for a utilization of air-stable materials for both electrodes and for an employment of thick and uneven active layers.<sup>37</sup> The latter two features are highly enabling from a low-cost solution-based processing perspective, and a roll-to-roll compatible slot-die coating fabrication of functional LEC sheets under uninterrupted ambient conditions was recently demonstrated.<sup>38</sup>

The first observation of white light emission from a LEC originated from Yang and Pei in 1997 and was attributed to phase separation between the electrolyte and the conjugated polymer;<sup>39</sup> other researchers have subsequently demonstrated broad-band white emission from primarily single-layer blend-emitter active-layers.<sup>40–46</sup> Here, we report on stable white light emission from a single-layer, single-emitter conformable LEC, comprising an MCP as the emitter sandwiched between two air-stable electrodes. We further present experimental data that indicate that the origin to the attained broad-band emission is the motion of ions within the active layer during the p–n junction formation and the related separation of the multifluorophoric emitting molecules, which in turn limits intermolecular interactions and related undesired energy-transfer processes. The proposed *in situ* ion-separating white-light facilitation is manifested in that an OLED, comprising the same MCP (that results in broad-band white emission in an LEC) but lacking the mobile ions, emits narrow-band red light.

**Received:** December 23, 2012

**Published:** February 11, 2013

## 2. EXPERIMENTAL SECTION

The multifluorophoric conjugated copolymer (MCP,  $M_w = 460,000$  g/mol,  $M_n = 151,000$  g/mol, synthesized by Merck, FRG), the ion-transport material trimethylolpropane ethoxylate (TMPE,  $M_n = 450$  g/mol, Aldrich, Steinheim, FRG) and the salt  $\text{LiCF}_3\text{SO}_3$  (Aldrich, Steinheim, FRG) were all used as received. The chemical structures of the MCP and the electrolyte are displayed in Figure 1a. For the LEC-

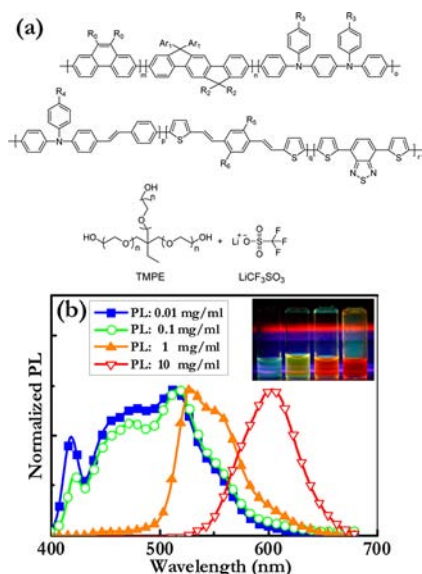


**Figure 1.** (a) Top: Chemical structure of the multifluorophoric conjugated copolymer (MCP);  $m + n + o + p + q + r = 1$ ;  $R_0$ ,  $R_2$ ,  $R_3$ , and  $R_4$  are solubilizing alkyl groups,  $Ar_1$  is an aryl group, and  $R_5$  and  $R_6$  are alkoxy groups. The molecular weight is  $M_w = 460$  kg/mol and  $M_n = 151$  kg/mol. Bottom: Chemical structure of the TMPE- $\text{LiCF}_3\text{SO}_3$  electrolyte. (b) UV-excited PL from the MCP in THF solution as a function of concentration. The inset shows photographs of the four different solutions under UV illumination in a dark room, with increasing concentration from left to right.

on-glass fabrication, poly(3,4-ethylenedioxythiophene)-poly(styrene sulfonate) (PEDOT:PSS, Clevios P VP AI 4083, Heraeus, FRG) was spin coated on top of carefully cleaned indium tin oxide (ITO)-coated glass substrates ( $1.5 \times 1.5$  cm<sup>2</sup>, 20  $\Omega$ /square, Thin Film Devices, USA) at 4000 rpm for 60 s. The resulting 40 nm thick PEDOT:PSS film was dried at  $T = 120$  °C for 6 h. The active material, comprising {MCP:TMPE: $\text{LiCF}_3\text{SO}_3$ } in a mass ratio of {1:0.1:0.03}, was spin-coated from a 10 mg/mL tetrahydrofuran (THF) solution at 2000 rpm for 60 s on top of the PEDOT:PSS layer in LEC-on-glass devices and directly on the flexible ITO-coated poly(ethylene terephthalate) (PET) substrates (PET60, 50  $\Omega$ /square, Visiotech Systems Ltd.) in LEC-on-plastic devices. The resulting 100 nm thick active material was dried at  $T = 50$  °C for  $\geq 5$  h. On top of the active layer, Al cathodes (thickness: 100 nm, area:  $0.85 \times 0.15$  cm<sup>2</sup>) were deposited by thermal evaporation at  $p < 2 \times 10^{-4}$  Pa through a shadow mask. For the OLED fabrication, the MCP was spin-coated on top of the PEDOT:PSS/ITO anode from a 10 mg/mL THF solution at 2000 rpm for 60 s. The resulting 100 nm thick MCP film was dried at  $T = 50$  °C for  $\geq 5$  h. The Ca cathodes, with an Al capping layer, were deposited on top of the MCP active layer by thermal evaporation to complete the OLED structure.

The devices were driven and measured by a Keithley 2400 source meter unit. The brightness was measured using a calibrated photodiode equipped with an eye response filter (Hamamatsu Photonics) and connected through a current-to-voltage amplifier to a HP 34401A voltmeter. Electroluminescence (EL) measurements were performed using a calibrated USB2000 fiber optic spectrometer (Ocean Optics). The color rendering index (CRI), the CIE coordinates, and the correlated color temperature (CCT) were

calculated using the SpectraWin software. The photoluminescence (PL) measurements were performed with a FP-6500 spectrofluorometer (JASCO). PL quantum efficiencies were measured with a calibrated integrating sphere connected to a fluorescence spectrometer (C-701, PTI, Photon Technology International), using a thin film of Tris-(8-hydroxyquinoline) aluminum as a reference. The energy levels of the MCP were established with cyclic voltammetry (CV), with a MCP-coated Au electrode as the working electrode, Pt as the counter electrode, and an Ag wire as the pseudoreference electrode. The electrolyte was 0.1 M tetrabutylammonium hexafluorophosphate dissolved in  $\text{CH}_3\text{CN}$ . The CV sweeps were driven and measured by an Autolab PGSTAT302 potentiostat. Directly after each CV scan, a calibration scan was run with a small amount of ferrocene added to the electrolyte. The onset potentials for oxidation and reduction were calculated as the intersection of the current baseline with the tangent of the current at the half-maximum of its peak value. Atomic force microscopy (AFM) images and film thicknesses were recorded using a MultiMode SPM microscope with a Nanoscope IV Controller (Veeco Metrology). All of the above procedures, except the cleaning of the substrates, the deposition of PEDOT:PSS, the PL measurement, and the AFM imaging, were carried out in two interconnected  $\text{N}_2$ -filled glove boxes ( $[\text{O}_2] < 3$  ppm,  $[\text{H}_2\text{O}] < 0.5$  ppm).

## 3. RESULTS AND DISCUSSION

Figure 1a depicts the chemical structure of the active layer constituents, while Figure 1b presents the PL spectra of MCP dissolved in THF over a broad concentration range. The latter results and the accompanying photographs of the UV-excited PL from the MCP solutions (see inset) reveal a strong dependence of the PL on MCP concentration. The most dilute 0.01 mg/mL MCP solution exhibits a broad PL spectrum, with three distinguishable peaks at:  $\sim 420$  nm (minor),  $\sim 475$  nm (intermediate), and  $\sim 515$  nm (major). With increasing concentration, the two higher-energy peaks first decrease in magnitude (0.1 mg/mL) and then completely disappear at 1 mg/mL, so that a markedly narrowed PL emission with a peak at  $\sim 530$  nm, and a shoulder at  $\sim 550$  nm, is detected. For the highest MCP concentration (10 mg/mL), a notably strong red shift results in a relatively symmetric and narrow PL emission centered at  $\lambda_{\text{peak}} \sim 605$  nm. As the MCP is designed to comprise three emitting species: 4-alkyl-N-phenyl-N-(4-styrylphenyl)-benzenamine; 1,4-bis(2-(thiophen-2-yl)vinyl)-3,6-bis(alkoxy)-benzene; and 4,7-bisthieryl-2,1,3-benzothiadiazole, which separately emit primarily blue, green, and red light, respectively,<sup>47</sup> we designate the 420–475 nm emission band as the “blue” segment, the 515–550 nm band as the “green” segment, and the  $\sim 605$  nm peak as the “red” segment. In the context of white light emission, it is obviously attractive that all three primary colors are available in the MCP PL.

With increasing MCP concentration, intermolecular (and possibly intramolecular) interactions will become more prominent, and it thus straightforward to attribute the observed strong bathochromic PL shift, and the line-width narrowing, to enlarged MCP aggregation. More specifically, with raised MCP concentration and aggregation, the excitons will be increasingly able to access (via diffusion or Förster transfer), and be trapped, at the lower-energy emitting segments on the MCP polymer; where they subsequently can decay by light emission. With the above observations in mind, and by convenience, we select to define an “isolated” MCP chain with limited energy-transfer interactions (exciton migration) as being a species that emits with high-energy blue and green light and an “aggregated” MCP chain with significant energy-transfer character as a species that emits with a low-energy red light.

We begin our device studies by implementing MCP as the emitting active layer sandwiched between an ITO/PEDOT:PSS anode and a calcium cathode in an OLED device. The energetics of this OLED at open circuit is shown in the inset of Figure 2a, and its optoelectronic response during a voltage-

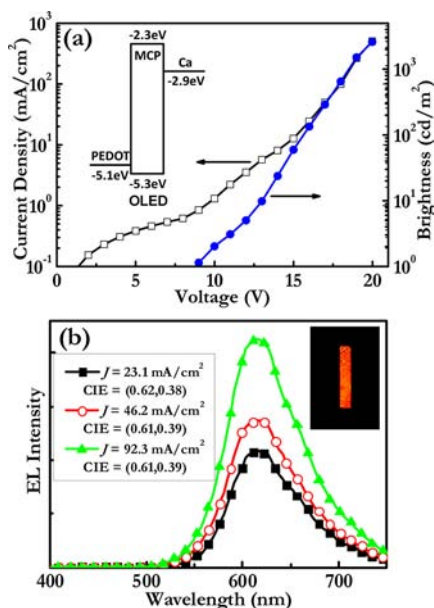


**Figure 2.** (a) The current density and brightness versus voltage for an OLED device with the following configuration: glass/ITO/PEDOT:PSS/MCP/Ca/Al. The scan rate was 1.0 V/s. The inset presents the energy levels of the OLED at open circuit. (b) EL spectra and color data as a function of drive current density. The inset presents a photograph of a red-emitting OLED device mounted on a glass substrate when driven at  $j = 23.1 \text{ mA/cm}^2$ .

ramp experiment is shown in Figure 2a. We measure a relatively modest performance in the form a high turn-on voltage [at a brightness ( $B$ ) of  $>1 \text{ cd/m}^2$ ] of 9 V, a maximum  $B$  of  $2600 \text{ cd/m}^2$  (at 20 V), and a maximum current efficacy of  $0.66 \text{ cd/A}$  (at  $B = 650 \text{ cd/m}^2$ ). Moreover, the EL spectra depicted in Figure 2b and the accompanying photograph in the inset reveal that we were not able to attain the desired broadband white light emission, as the emission from the higher-energy “blue” and “green” MCP segments is completely quenched. Instead, the OLED device emits solely red light at  $\lambda_{\text{peak}} = 614 \text{ nm}$  at all investigated drive current densities (and drive voltages; the latter data not shown). Thus, the conclusions are that effectively all MCP polymer chains are in the aggregated state and that the excitons created on the higher-energy blue and green segments are funneled to the lowest-energy red segment in a highly efficient energy-transfer process; see Figure 3a for a schematic representation of our proposed scenario in effect in the emission zone of a biased OLED device.

With the disappointing OLED performance in mind, particularly the apparently detrimental strong aggregation of the MCP chains, we turn our attention to the LEC device configuration. The LEC is distinct from the OLED in that it contains mobile ions, which redistribute when a voltage is applied during device operation. The anions drift to the anode and the cations drift to the cathode to facilitate the initial electronic charge injection. The first holes/electrons injected at the anode/cathode attract compensating anions/cations from the electrolyte in a doping process, termed p-type at the anode

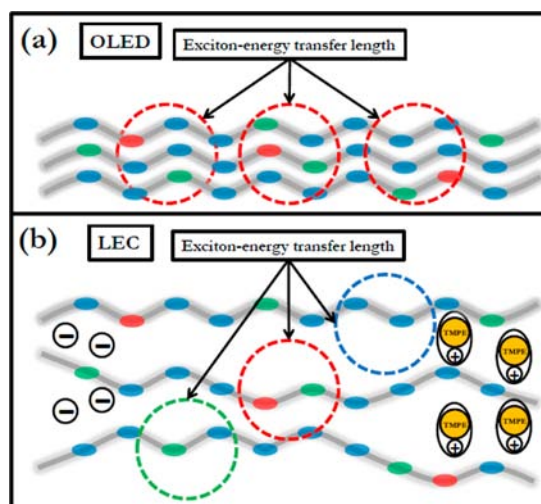


**Figure 3.** (a) Schematic illustrating the aggregated MCP chains in an OLED, which result in efficient intermolecular energy transfer and narrow emission from the low-energy (red) fluorophores. (b) Schematic depicting the ion-induced separation of MCP chains in an LEC during operation. The partial MCP separation in the emission zone (the p–n junction) in the LEC allows for a broad-band combination of “aggregated” (red) and “isolated” (blue and green) emission.

and n-type at the cathode. With time the p- and n-type doping regions grow in size to finally make contact in the bulk of the active layer under the formation of a p–n junction. At this junction subsequently injected electrons and holes will recombine to form excitons, which can probe (via diffusion or Förster transfer), on average, one exciton-energy transfer length before decaying radiatively (and nonradiatively).

Our hypothesis is that this ion-migration process can provide separation of the MCP chains, so that it is possible to harvest exciton emission also from “isolated” MCP chains, with the result being that broadband white EL can be recorded. More specifically, in consideration of the high doping levels in effect in LECs ( $\sim 0.1$  dopants/monomer),<sup>48</sup> that each dopant is concomitant with an ion being positioned in very close proximity of a MCP chain and that the selected electrolyte features a big  $\text{CF}_3\text{SO}_3$  anion and a bulky, coordinated  $\text{Li}^+$ -TMPE cation-solvent complex (see Figure 1a),<sup>49</sup> we anticipate that the MCP chains will be efficiently separated on a molecular level in the doping regions. We further anticipate that this ion-induced separation of the MCP chains will partially carry over into the relatively dopant-free p–n junction, where the excitons form, on the merit of its thinness (impedance spectroscopy studies indicate a thickness of the order of  $\sim 10 \text{ nm}$ )<sup>50</sup> and the high molecular weight (long average chain length) of the MCP polymer. Figure 3b presents our anticipated and desired scenario with a partial ion-induced MCP separation in the emission zone, which results in a combination of “aggregated” red EL and “isolated” green and blue EL.

Figure 4a shows the temporal optoelectronic response during galvanostatic (constant current) operation of an LEC device, comprising a blend of MCP and a  $\text{LiCF}_3\text{SO}_3$ -TMPE electrolyte as the active layer sandwiched between an Al cathode and an ITO/PEDOT:PSS anode. The LEC functionality is manifested in an increase in brightness and a decrease in driving voltage, during the initial doping process, and a good performance despite the employment of an air-stabile Al cathode (with a concomitant large injection barrier for electron injection; see

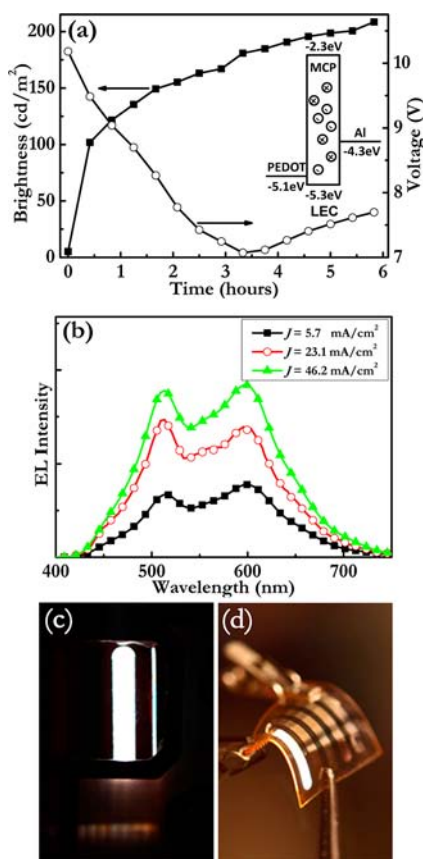


**Figure 4.** (a) The temporal response of an LEC device with the following configuration: glass/ITO/PEDOT:PSS/{MCP+TMPE+LiCF<sub>3</sub>SO<sub>3</sub>}/Al. The device was driven in galvanostatic mode at  $j = 5.7$  mA/cm<sup>2</sup>. The inset presents the energy levels of the LEC device at open circuit. (b) EL spectra recorded as a function of current density for the same LEC. Photographs depicting the white emission at  $j = 5.7$  mA/cm<sup>2</sup> from an LEC device mounted on (c) a glass substrate and (d) a flexible PET substrate.

inset in Figure 4a for device energetics at open circuit). Specifically, we measure a current conversion efficacy and power conversion efficacy of 3.8 cd/A and 1.2 lm/W (at  $B = 220$  cd/m<sup>2</sup>), respectively, a maximum brightness of 6240 cd/m<sup>2</sup> at  $V = 9.5$  V, and an operational lifetime of 52 h (at  $B \geq 100$  cd/m<sup>2</sup>). The device in Figure 4a was fabricated on a rigid glass substrate, but a similar performance was attained on devices fabricated on flexible PET substrates.

Most importantly, however, is that the LECs emit white light! Figure 4b shows the broad-band EL spectrum from an LEC device as a function of drive current density ( $j$ ), and Figure 4c,d shows photographs of the light emission from a rigid LEC-on-glass device and a flexed LEC-on-plastic device, respectively. The quality of the white light is quantified by measured CIE coordinates of (0.41, 0.45), a color rendering index (CRI) of 82, and a correlated color temperature (CCT) of 4000 K. As a reference, we mention that indoor lighting applications typically require a CRI value of 80 or larger<sup>51</sup> and that a light bulb emits with a CCT of  $\sim 3000$  K and the sun with  $\sim 5000$ – $6000$  K (depending on its position in the sky). The MCP-LECs thus emit with a warm-light appearance. It is further notable that the EL spectrum is unaffected by variations in drive current (and drive voltage), as exemplified by Figure 4b and as demonstrated by minute shifts in the color metrics recorded over the investigated wide drive current-density range

( $5.7 \leq j \leq 46.2$  mA/cm<sup>2</sup>). The latter is obviously an important feature for a practical solid-state lighting device.

For many applications, the efficiency is a fundamental factor, and an insight into how it can be further improved follows from an analysis of the constituent factors in the equation for the external quantum efficiency ( $\eta_{\text{ext}}$ ):

$$\eta_{\text{ext}} = \eta_{\text{rec}} \times \eta_{\text{ST}} \times \eta_{\text{PL}} \times \eta_{\text{out}} \times X_{\text{loss}} \quad (1)$$

where  $\eta_{\text{rec}}$  is the ratio of the number of exciton formation events within the device to the number of electrons flowing in the external circuit,  $\eta_{\text{ST}}$  is the fraction of excitons that are formed as singlets,  $\eta_{\text{PL}}$  is the PL quantum efficiency of the emitter, and  $\eta_{\text{out}}$  is the out-coupling efficiency of the device structure.  $X_{\text{loss}}$  is a factor that represents the combined additional loss mechanisms, due to, e.g., exciton–dopant, exciton–exciton, and exciton–electrode quenching, which can be improved by an adjustment of the doping structure.  $\eta_{\text{ext}}$  was calculated to be 0.016 using the measured current conversion efficiency and the EL spectrum,<sup>52</sup> while  $\eta_{\text{rec}}$  and  $\eta_{\text{ST}}$  were set to 1 and 0.25, respectively, in consideration of the effective electron–hole recombination in a p–n homojunction and the generic singlet–triplet branching ratio in conjugated polymers. The PL quantum efficiency of a pristine MCP film and an {MCP + TMPE + LiCF<sub>3</sub>SO<sub>3</sub>} film, as employed in the LEC devices, was measured to be 0.276 and 0.248, respectively, and we selected the former value for  $\eta_{\text{PL}}$  since the emission zone is anticipated to comprise a very small amount of electrolyte during light emission (see Figure 3b). The value for  $\eta_{\text{out}}$  was estimated to be  $\sim 0.22$  following the procedure outlined in refs 53 and 54 and assuming a value for the refractive index of MCP of 1.5. With this information at hand, we calculate that  $X_{\text{loss}} = 1.0$ . In other words, the *in situ* formed p–n junction must be considered a highly efficient doping structure, in that the formed excitons are left unaffected by nearby dopants, other excitons, and the electrodes. This analysis further implies that future efforts toward improving the device efficiency should be focused on the development of materials with higher PL quantum efficiencies, the introduction of triplet emitters, and on the inclusion of appropriate out-coupling structures.

We finally attempt to further explain the mechanism in effect behind our light emission results with the aid of an expanded PL and EL investigation. Figure 5a presents the PL from a dilute and a highly concentrated MCP solution, where the former PL has been designated as “isolated” MCP emission and the latter as “aggregated” MCP emission (see also Figure 1b and related discussion). Figure 5b shows the PL and EL spectra from the MCP film in an OLED and from the {MCP + electrolyte} film in an LEC device.

We note that the MCP-film/OLED PL (black squares, Figure 5b) is more structured than the concentrated MCP-solution PL (open red circles, Figure 5a), as it exhibits distinct green and blue shoulders at shorter wavelengths that are absent in the concentrated solution. This implies that the downward energy transfer to the red segment is more effective in the concentrated MCP solution than in the MCP film. We attribute this observation to the faster polymer dynamics in solution and speculate that the downward energy transfer to the low-content ( $\leq 1$  mass %) red-emitting fluorophore is dependent on a specific conformation that is more probable in the dynamic liquid phase than in the static solid phase.

With addition of the TMPE-LiCF<sub>3</sub>SO<sub>3</sub> electrolyte to the MCP film (OLED  $\rightarrow$  LEC), the structured PL emission becomes even more pronounced (compare open red circles

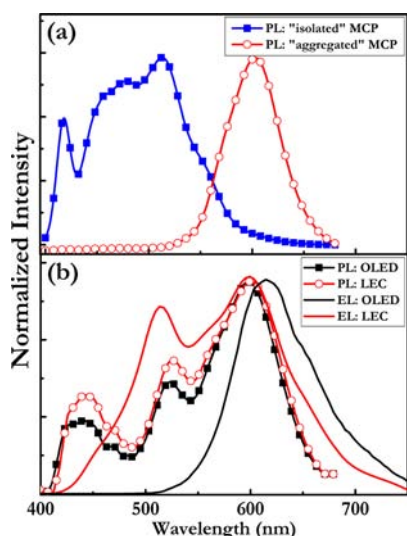


**Figure 5.** (a) Normalized PL spectra for the MCP dissolved in THF at low (0.01 mg/mL, solid blue squares) and high (10 mg/mL, open red circles) MCP concentration. (b) Normalized PL and EL spectra from OLED and LEC films.

with solid black squares, Figure 5b); the blue and green shoulders are also observed to increase in relative magnitude with increasing electrolyte concentration (data not shown). This suggests that the electrolyte assists in hindering the energy transfer from the high-energy blue and green segments to the low-energy red segment, presumably by separating the MCP chains from each other (and/or further prohibiting them from adopting a conformation prone to energy transfer). In this context, we point out that an AFM study revealed that the ion-containing electrolyte and the MCP are phase separated on the  $\sim 50$ -nm scale in the nonbiased LEC (data not shown) and that this type of ion-induced MCP separation in the nonbiased LEC as a consequence is not expected to be particularly efficient.

A key observation in Figure 5b is that the difference in emission from the LEC and the OLED films is much more pronounced in the EL (compare solid lines) than in the PL (compare symbols). This supports our hypothesis that the unique *in situ* doping process in effect in an LEC, during which ions penetrate in between the MCP polymer chains, is the main factor that transforms the MCP emission from red in the OLED to turn white in the LEC; compare the two schematics in Figure 3a,b for a visualization of the proposed ion-separation process. We also wish to call attention to that while charge trapping during electric transport rationalizes the observed minor red-shift in going from OLED PL ( $\lambda_{\text{peak}} = 600$  nm) to OLED EL ( $\lambda_{\text{peak}} = 615$  nm), it cannot explain the significant blue-broadening in going from PL to EL in the LEC. We finally note that the LEC EL exhibits peaks at both 514 and 600 nm, which are almost identical with the “isolated” PL peak at 515 nm and the “aggregated” PL peak at 604 nm (see Figure 5a); thus corroborating our hypothesis that the white EL from an LEC indeed stems from a combination of ion-separated isolated and aggregated MCP chains.

#### 4. CONCLUSIONS

To summarize, we present a practical single-layer, single-emitter LEC device that emits broad-band white light, with a color rendering index of 82, a correlated-color temperature of 4000 K, and a current conversion efficacy of 3.8 cd/A. The quality of

the white light emission is, as expected from a single-emitter configuration, demonstrated to be effectively independent of the drive current and voltage. We demonstrate that the enabling factor for the white light emission is the employment of a multifluorophoric conjugated polymer, which exhibits broad-band emission capacity in diluted form, and an electrolyte capable of separating the polymer chains during the *in situ* doping process in effect in LECs. With this in mind, we believe that we have demonstrated a generic approach for attaining stable white light from an LEC device, which might become applicable in future solid-state lighting and display applications.

#### AUTHOR INFORMATION

##### Corresponding Author

ludvig.edman@physics.umu.se

##### Notes

The authors declare no competing financial interest.

#### ACKNOWLEDGMENTS

We wish to thank Dr. Xueen Jia for assistance with the PL measurement. We are also grateful to the Swedish Research Council, Energimyndigheten, Kempestiftelserna, and Carl Trygger's foundation for financial support. L.E. is a “Royal Swedish Academy of Sciences Research Fellow” supported by a grant from the Knut and Alice Wallenberg Foundation.

#### REFERENCES

- (1) Tang, C. W.; Vanslyke, S. A. *Appl. Phys. Lett.* **1987**, *51*, 913–915.
- (2) Pei, Q. B.; Yu, G.; Zhang, C.; Yang, Y.; Heeger, A. J. *Science* **1995**, *269*, 1086–1088.
- (3) D'Andrade, B. W.; Thompson, M. E.; Forrest, S. R. *Adv. Mater.* **2002**, *14*, 147–151.
- (4) Sun, Y.; Giebink, N. C.; Kanno, H.; Ma, B.; Thompson, M. E.; Forrest, S. R. *Nature* **2006**, *440*, 908–912.
- (5) Kido, J.; Kimura, M.; Nagai, K. *Science* **1995**, *267*, 1332–1334.
- (6) D'Andrade, B. W.; Holmes, R. J.; Forrest, S. R. *Adv. Mater.* **2004**, *16*, 624–628.
- (7) Kido, J.; Hongawa, K.; Okuyama, K.; Nagai, K. *Appl. Phys. Lett.* **1994**, *64*, 815–817.
- (8) Gong, X.; Ma, W.; Ostrowski, J. C.; Bazan, G. C.; Moses, D.; Heeger, A. J. *Adv. Mater.* **2004**, *16*, 615–619.
- (9) Wu, H. B.; Zou, J. H.; Liu, F.; Wang, L.; Mikhailovsky, A.; Bazan, G. C.; Yang, W.; Cao, Y. *Adv. Mater.* **2008**, *20*, 696–702.
- (10) Xu, Q.; Duong, H. M.; Wudl, F.; Yang, Y. *Appl. Phys. Lett.* **2004**, *85*, 3357–3359.
- (11) Reineke, S.; Lindner, F.; Schwartz, G.; Seidler, N.; Walzer, K.; Lussem, B.; Leo, K. *Nature* **2009**, *459*, 234–238.
- (12) Huang, J.; Li, G.; Wu, E.; Xu, Q.; Yang, Y. *Adv. Mater.* **2006**, *18*, 114–117.
- (13) Tokito, S.; Suzuki, M.; Sato, F.; Kamachi, M.; Shirane, K. *Org. Electron.* **2003**, *4*, 105–111.
- (14) Shih, P. I.; Tseng, Y. H.; Wu, F. I.; Dixit, A. K.; Shu, C. F. *Adv. Funct. Mater.* **2006**, *16*, 1582–1589.
- (15) Berggren, M.; Inganäs, O.; Gustafsson, G.; Rasmussen, J.; Andersson, M. R.; Hjertberg, T.; Wennerstrom, O. *Nature* **1994**, *372*, 444–446.
- (16) Tasch, S.; List, E. J. W.; Ekstrom, O.; Graupner, W.; Leising, G.; Schlichting, P.; Rohr, U.; Geerts, Y.; Scherf, U.; Mullen, K. *Appl. Phys. Lett.* **1997**, *71*, 2883–2885.
- (17) Kido, J.; Shionoya, H.; Nagai, K. *Appl. Phys. Lett.* **1995**, *67*, 2281–2283.
- (18) Granström, M.; Inganäs, O. *Appl. Phys. Lett.* **1996**, *68*, 147–149.
- (19) Lee, S. K.; Hwang, D. H.; Jung, B. J.; Cho, N. S.; Lee, J.; Lee, J. D.; Shim, H. K. *Adv. Funct. Mater.* **2005**, *15*, 1647–1655.

- (20) Luo, J.; Li, X.; Hou, Q.; Peng, J. B.; Yang, W.; Cao, Y. *Adv. Mater.* **2007**, *19*, 1113–1117.
- (21) Liu, J.; Zhou, Q. G.; Cheng, Y. X.; Geng, Y. H.; Wang, L. X.; Ma, D. G.; Jing, X. B.; Wang, F. S. *Adv. Mater.* **2005**, *17*, 2974–2978.
- (22) Jiang, J. X.; Xu, Y. H.; Yang, W.; Guan, R.; Liu, Z. Q.; Zhen, H. Y.; Cao, Y. *Adv. Mater.* **2006**, *18*, 1769–1773.
- (23) Zhen, H.; Xu, W.; Yang, W.; Chen, Q.; Xu, Y.; Jiang, J.; Peng, J.; Cao, Y. *Macromol. Rapid Commun.* **2006**, *27*, 2095–2100.
- (24) Tu, G. L.; Mei, C. Y.; Zhou, Q. G.; Cheng, Y. X.; Geng, Y. H.; Wang, L. X.; Ma, D. G.; Jing, X. B.; Wang, F. S. *Adv. Funct. Mater.* **2006**, *16*, 101–106.
- (25) Liu, J.; Zhou, Q. G.; Cheng, Y. X.; Geng, Y. H.; Wang, L. X.; Ma, D. G.; Jing, X. B.; Wang, F. S. *Adv. Funct. Mater.* **2006**, *16*, 957–965.
- (26) Chen, L.; Li, P.; Cheng, Y.; Xie, Z.; Wang, L.; Jing, X.; Wang, F. *Adv. Mater.* **2011**, *23*, 2986–2990.
- (27) Edman, L. *Electrochim. Acta* **2005**, *50*, 3878–3885.
- (28) Leger, J. M.; Rodovsky, D. B.; Bartholomew, G. R. *Adv. Mater.* **2006**, *18*, 3130–3134.
- (29) Shao, Y.; Bazan, G. C.; Heeger, A. J. *Adv. Mater.* **2007**, *19*, 365–370.
- (30) Gao, J.; Yu, G.; Heeger, A. J. *Appl. Phys. Lett.* **1997**, *71*, 1293–1295.
- (31) deMello, J. C.; Halls, J. J. M.; Graham, S. C.; Tessler, N.; Friend, R. H. *Phys. Rev. Lett.* **2000**, *85*, 421.
- (32) Costa, R. D.; Ortí, E.; Bolink, H. J.; Monti, F.; Accorsi, G.; Armaroli, N. *Angew. Chem. Int. Ed.* **2012**, *51*, 8178–8211.
- (33) Tordera, D.; Meier, S.; Lenes, M.; Costa, R. D.; Ortí, E.; Sarfert, W.; Bolink, H. J. *Adv. Mater.* **2012**, *24*, 897–900.
- (34) Matyba, P.; Maturova, K.; Kemerink, M.; Robinson, N. D.; Edman, L. *Nat. Mater.* **2009**, *8*, 672–676.
- (35) Pei, Q.; Heeger, A. J. *Nat. Mater.* **2008**, *7*, 167–167.
- (36) Lenes, M.; Garcia-Belmonte, G.; Tordera, D.; Pertegás, A.; Bisquert, J.; Bolink, H. J. *Adv. Funct. Mater.* **2011**, *21*, 1581–1586.
- (37) Matyba, P.; Yamaguchi, H.; Eda, G.; Chhowalla, M.; Edman, L.; Robinson, N. D. *ACS Nano* **2010**, *4*, 637–642.
- (38) Sandström, A.; Dam, H. F.; Krebs, F. C.; Edman, L. *Nat. Commun.* **2012**, *3*, 1002.
- (39) Yang, Y.; Pei, Q. *J. Appl. Phys.* **1997**, *81*, 3294–3298.
- (40) Sun, M.; Zhong, C.; Li, F.; Cao, Y.; Pei, Q. *Macromolecules* **2010**, *43*, 1714–1718.
- (41) Tang, S.; Pan, J.; Buchholz, H.; Edman, L. *ACS Appl. Mater. Interfaces* **2011**, *3*, 3384–3388.
- (42) He, L.; Qiao, J.; Duan, L.; Dong, G.; Zhang, D.; Wang, L.; Qiu, Y. *Adv. Funct. Mater.* **2009**, *19*, 2950–2960.
- (43) Su, H.-C.; Chen, H.-F.; Fang, F.-C.; Liu, C.-C.; Wu, C.-C.; Wong, K.-T.; Liu, Y.-H.; Peng, S.-M. *J. Am. Chem. Soc.* **2008**, *130*, 3413–3419.
- (44) He, L.; Duan, L.; Qiao, J.; Dong, G.; Wang, L.; Qiu, Y. *Chem. Mater.* **2010**, *22*, 3535–3542.
- (45) Wu, H.-B.; Chen, H.-F.; Liao, C.-T.; Su, H.-C.; Wong, K.-T. *Org. Electron.* **2012**, *13*, 483–490.
- (46) He, L.; Duan, L.; Qiao, J.; Zhang, D.; Wang, L.; Qiu, Y. *Org. Electron.* **2010**, *11*, 1185–1191.
- (47) Meyer, F. E.; Schulte, N.; Kreuder, W. U.S. Patent 20110095280, April 28, 2011.
- (48) Shin, J. H.; Robinson, N. D.; Xiao, S.; Edman, L. *Adv. Funct. Mater.* **2007**, *17*, 1807–1813.
- (49) Tang, S.; Edman, L. *J. Phys. Chem. Lett.* **2010**, *1*, 2727–2732.
- (50) Munar, A.; Sandström, A.; Tang, S.; Edman, L. *Adv. Funct. Mater.* **2012**, *22*, 1511–1517.
- (51) *Lighting Handbook*, 8th ed.; IESNA: New York, 1993.
- (52) Forrest, S. R.; Bradley, D. D. C.; Thompson, M. E. *Adv. Mater.* **2003**, *15*, 1043–1048.
- (53) Madigan, C. F.; Lu, M. H.; Sturm, J. C. *Appl. Phys. Lett.* **2000**, *76*, 1650–1652.
- (54) Gu, G.; Garbuzov, D. Z.; Burrows, P. E.; Venkatesh, S.; Forrest, S. R.; Thompson, M. E. *Opt. Lett.* **1997**, *22*, 396–398.